ChemComm

COMMUNICATION

View Article Online
View Journal | View Issue

Cite this: *Chem. Commun.*, 2021, **57**, 2800

Received 6th December 2020,
Accepted 27th January 2021

DOI: 10.1039/d0cc07930h

rsc.li/chemcomm

A near-infrared fluorogenic probe for nuclear thiophenol detection†

Jinye Niu,‡[ab] Yong Li,‡[a] Ran Zhang,[a] Jian Zhang,[a] Xu Wang,*[a] Xilei Xie,[a] Xiaoyun Jiao[a] and Bo Tang *[a]

Based on the thiolysis of dinitrophenyl ethers, a nucleus-targeted fluorescent probe, AQD, with bisalkylaminoanthraquinone as the fluorophore, was prepared for the near-infrared mapping of thiophenol in live cells, zebrafish, and mice.

Thiophenol is a crucial raw material and intermediate that has been extensively employed in the manufacture of pharmaceuticals, agrochemicals, polymeric materials, and so on.[1] However, in spite of its broad synthetic utility, thiophenol is highly poisonous to organisms,[2] and has been evaluated as a No. P014 acute hazardous pollutant by the united states environment protection agency.[3] Moreover, thiophenol can be easily absorbed in organisms *via* inhalation and the skin, and the prolonged exposure to thiophenol tends to induce various human health issues, such as central nerve injury, nausea, muscle weakness, cough, and even death.[4] The cytotoxic mechanism study demonstrated that DNA damage has been deeply involved in thiophenol-induced biotoxic events.[5] Therefore, considering that nucleus is the main subcellular location of the eukaryotic cell DNA, the fabrication of a superior performance strategy for thiophenol tracing in cellular nucleus is undoubtedly significant in the field of biotoxic evaluation of thiophenol.

Currently, fluorescence detection, especially, near-infrared imaging, is widely utilized to track various active molecules *in vitro* and *in vivo* by virtue of its unique spatiotemporal resolution, noninvasive capacity, and so on.[6] Accordingly, much efforts have been made to construct fluorescent probes for thiophenol monitoring with satisfactory response behaviors.[7] However, challenges exist as none of the fluorescent probes reported so far were capable of accomplishing thiophenol specific sensing in cellular nucleus.

Herein, based on the thiolysis of dinitrophenyl ethers, we established a near-infrared bisalkylaminoanthraquinone–dinitrobenzene conjugate, **AQD**, for nuclear thiophenol detection with prominent sensitivity and specificity. By capitalizing on outstanding response features of **AQD**, the nuclear thiophenol level fluctuations in HeLa cells, zebrafish, and mice were successfully revealed. This work not only provided a potent probe for thiophenol detection but also afforded information that may contribute to the intensive understanding of thiophenol cytotoxic mechanism, especially that in cell nucleus.

The unique probe, **AQD**, was fabricated by integrating dinitrophenyl groups into bisalkylaminoanthraquinone (**AQ**) through an ether linker, in which the dinitrophenyl group was introduced both as a thiophenol trigger and a fluorescence quencher while **AQ** was employed as a near-infrared fluorescent reporter and a nucleus-targeted unit.[8] In the absence of thiophenol, the fluorescence of **AQD** is supposed to be silenced by the strong photoinduced electron transfer (PET) effect of the dinitrophenyl group. Upon thiophenol exposure, the ether bond would be first cut off, and then the PET effect relieves, thus switching on the fluorescence of **AQD**. Simultaneously, the weakened intramolecular charge transfer (ICT) induced by an electron-withdrawing dinitrophenyl group would eliminate upon thiophenol recognition (Scheme 1). **AQD** was readily prepared and its structure was well characterized by high resolution mass spectrometry (HRMS), ^{1}H NMR, and ^{13}C NMR analysis (ESI†).

With **AQD** in hand, its spectral response towards thiophenol was first investigated. After thiophenol incubation, an obvious bathochromic-shift (60 nm) of the maximum absorption band was obtained, thus exhibiting the effective ICT recovery caused by the thiolysis of the dinitrophenyl group (Fig. S1, ESI†). Concomitantly, the distinct colorimetric change (purple to blue)

[a] *College of Chemistry, Chemical Engineering and Materials Science, Collaborative Innovation Center of Functionalized Probes for Chemical Imaging in Universities of Shandong, Key Laboratory of Molecular and Nano Probes, Ministry of Education, Shandong Provincial Key Laboratory of Clean Production of Fine Chemicals, Shandong Normal University, Jinan 250014, P. R. China. E-mail: tangb@sdnu.edu.cn, wangxu@sdnu.edu.cn*

[b] *School of Chemical Engineering, Shandong University of Technology, Zibo 255049, P. R. China*

† Electronic supplementary information (ESI) available: Experimental details, supplementary data, synthesis and characterization of compounds. See DOI: 10.1039/d0cc07930h

‡ These authors contributed equally to this work.

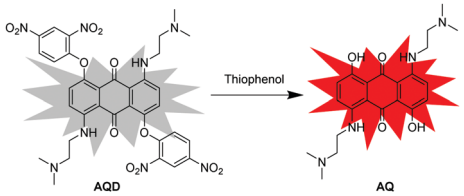

Scheme 1 Chemical structure of **AQD** and the proposed response mechanism for thiophenol.

in Fig. S1 (ESI†) hinted **AQD**'s naked-eye response capacity toward thiophenol. Meanwhile, as shown in Fig. 1, the treatment of **AQD** with an equivalent of thiophenol displayed a dramatic fluorescence increment (39 folds) with the maximum emission band at around 680 nm, presenting effective PET effect elimination. In addition, the fluorescence intensity of **AQD** showed a concentration-dependent augmentation towards thiophenol with a linear relationship of $y = 49.5221 + 427.5985x$ ([thiophenol] = 0–3.0 μM, $R^2 = 0.993$) and $y = 1057.6457 + 67.7261x$ ([thiophenol] = 3.0–10 μM, $R^2 = 0.991$), respectively. And the limit of detection was calculated as 15 nM based on $3\sigma/k$. Meanwhile, the time-dependent fluorescence variation of **AQD** with reaction time was assessed (Fig. S2, ESI†). After exposure to an equivalent of thiophenol, the fluorescence intensity of **AQD** displayed a sharp enhancement (35 folds) within 12 min, and then fully saturated (39 folds) after 60 min. Taken together, these results suggested that **AQD** was capable of tracking thiophenol with high sensitivity and reaction activity.

The proposed reaction mechanism between **AQD** and thiophenol was explored *via* HRMS. Upon thiophenol incubation, the **AQD** solution showed a discriminable mass peak at *m*/*z* 413.2162 $[M + H]^+$, which was in good agreement with compound **AQ** (Fig. S3, ESI†). This observation presented high consistence with the proposed thiophenol reaction pathway as shown in Scheme 1.

The specificity of **AQD** towards thiophenol was estimated (Fig. 2). Satisfactorily, no obvious fluorescence intensity change was triggered when **AQD** was incubated with a panel of reactive sulfur species, such as cysteine (Cys), glutathione (GSH), homocysteine (Hcy), hydrogen sulfide (H_2S), and bisulfite (HSO_3^-). The specificity of **AQD** towards thiophenol over other biothiols

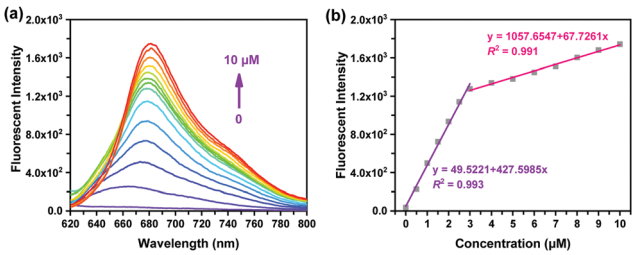

Fig. 1 (a) Fluorescence spectra variation of **AQD** (10 μM) with the addition of increasing amount of thiophenol (0–10 μM). (b) Linear correlation between the fluorescence intensity of **AQD** at 680 nm and thiophenol concentration. The results were recorded after incubation of **AQD** with thiophenol for 60 min in HEPES buffer (20 mM, pH 7.4, 30% DMSO) at 37 °C. λ_{ex} = 600 nm. Slit width: 5 nm/5 nm.

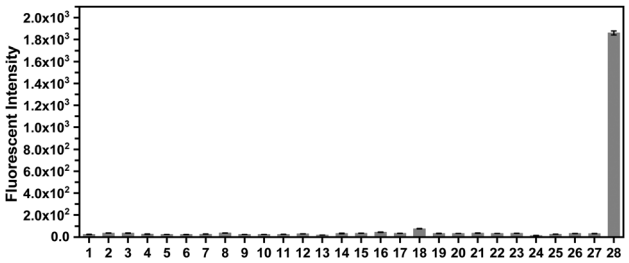

Fig. 2 The specificity of **AQD** (10 μM) towards various bioanalytes: 1. Blank; 2. Cys; 3. GSH; 4. Hcy; 5. HS^-; 6. HSO_3^-; 7 Vc.; 8. $ONOO^-$; 9. NO; 10. H_2O_2; 11. ClO^-; 12. $^1O_2$; 13. $^\bullet OH$; 14. $O_2^{\bullet-}$; 15. Na^+; 16. K^+; 17. Cd^{2+}; 18. Pd^{2+}; 19. Co^{2+}; 20. Mg^{2+}; 21. Hg^{2+}; 22. Ca^{2+}; 23. Zn^{2+}; 24. Cu^{2+}; 25. Fe^{2+}; 26. Al^{3+}; 27. Fe^{3+}; 28. Thiophenol (10 μM). The concentrations of GSH, Hcy, and Cys were 1.0 mM, the concentrations of metal ions were 500 μM, and the concentrations of the other substances were 100 μM unless otherwise stated. The results were recorded after incubation of **AQD** with various substances for 60 min in HEPES buffer (20 mM, pH 7.4, 30% DMSO) at 37 °C. $\lambda_{ex}/\lambda_{em}$ = 600/680 nm. Slit width: 5 nm/5 nm.

was probably due to the fact that fluorophore **AQ** decreased the electrophilicity of the 2,4-dinitrophenyl ether unit and thus **AQD** could be only attacked by the stronger nucleophile thiophenol.[9] In addition, negligible fluorescence enhancement was observed after treatment of **AQD** with other common active substances, including reactive nitrogen and reactive oxygen species ($ONOO^-$, NO, H_2O_2, ClO^-, $^1O_2$, $^\bullet OH$, and $O_2^{\bullet-}$), and metal ions (Na^+, K^+, Cd^{2+}, Pd^{2+}, Co^{2+}, Mg^{2+}, Hg^{2+}, Ca^{2+}, Zn^{2+}, Cu^{2+}, Fe^{2+}, Al^{3+}, and Fe^{3+}), thus implying the high specificity of **AQD** towards thiophenol. After that, the effect of pH on fluorescence response behavior of **AQD** was examined (Fig. S4, ESI†). It can be found that **AQD** itself showed weak and constant fluorescence emission at the wide pH range 3.0–10.0. In the presence of thiophenol, strong fluorescent signals were detected in the pH range 5.0–8.0, demonstrating that **AQD** can work effectively in biological specimen.

Encouraged by **AQD**'s outstanding thiophenol recognition behaviors, the imaging profile of **AQD** in the living system was exploited next. Prior to cell imaging, the high biocompatibility (IC_{50} = 207 μM) of **AQD** was well verified through MTT assays (Fig. S5, ESI†). Subsequently, the time-dependent thiophenol imaging in living cells was performed. The HeLa cells were pretreated with thiophenol followed by staining with **AQD** and then imaged immediately. With the passage of incubation time, the increased fluorescence intensity appeared gradually and significantly, and reached the maximum at 40 min (Fig. 3 and Fig. S6, ESI†), thus displaying that **AQD** can effectively capture thiophenol in the living system within 40 min. After that, the thiophenol dose-dependent fluorescence changes were explored. As can be seen from Fig. 4, the HeLa cells loaded with **AQD** alone emitted a negligible fluorescence signal, hinting that there is no thiophenol in living cells. Contrastingly, a remarkable increased fluorescence in cells appeared upon thiophenol administration. And the increment in fluorescence intensity displayed a positive relation with the dose of thiophenol. Furthermore, the cells co-stained with **AQD** and DAPI, a commercially available nuclear marker, led to an excellent colocalization with a high Pearson's correlation of 0.91 (Fig. S7, ESI†),

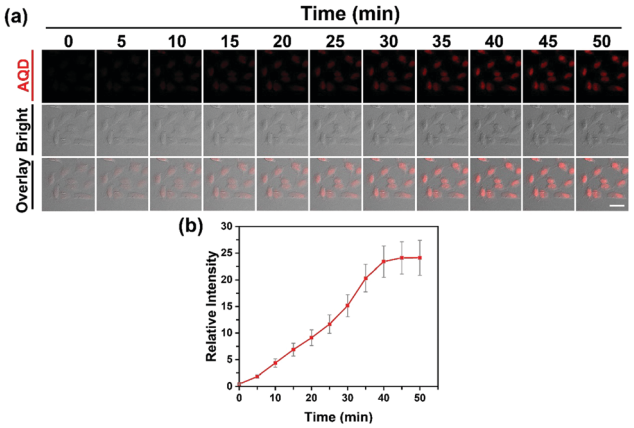

Fig. 3 Time-dependent fluorescence imaging of **AQD** in HeLa cells. (a) The cells were pretreated with thiophenol (10 μM) for 15 min and then incubated with **AQD** (10 μM) followed by imaging at different time points (0, 5, 10, 15, 20, 25, 30, 35, 40, 45, and 50 min); (b) the relative fluorescence intensity of (a). The images were recorded with 633 nm excitation and 640–730 nm collection. Scale bar = 20 μm.

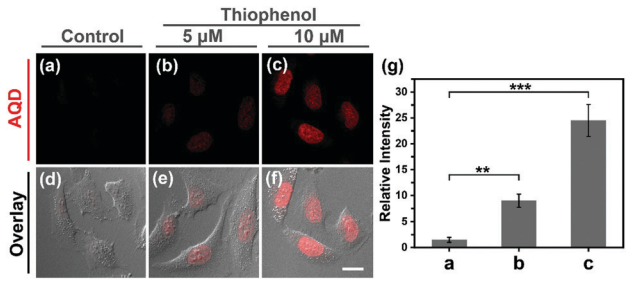

Fig. 4 Confocal fluorescence imaging of thiophenol in HeLa cells. (a and d) The cells were incubated with **AQD** (10 μM) only for 60 min; (b and e) the cells were pretreated with thiophenol (5 μM) for 15 min, and then incubated with **AQD** for 60 min; (c and f) the cells were pretreated with thiophenol (10 μM) for 15 min and further stained with **AQD** for 60 min. (g) The relative fluorescence intensity of (a–c). The images were recorded with 633 nm excitation and 640–730 nm collection. The values are the mean ± s.d. for n = 3, $^{**}p < 0.01$, and $^{***}p < 0.001$. Scale bar = 20 μm.

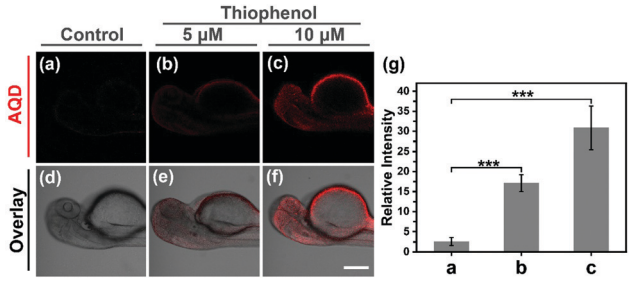

Fig. 5 Confocal fluorescence imaging of thiophenol in zebrafish. (a and d) The zebrafish was incubated with **AQD** (10 μM) only for 60 min; (b and e) the zebrafish was pretreated with thiophenol (5 μM) for 15 min, and then incubated with **AQD** for 60 min; (c and f) the zebrafish was administrated with thiophenol (10 μM) for 15 min and further stained with **AQD** for 60 min. (g) The relative fluorescence intensity of (a–c). The images were recorded with 633 nm excitation and 640–730 nm collection. The values are the mean ± s.d. for n = 3 and $^{***}p < 0.001$. Scale bar = 250 μm.

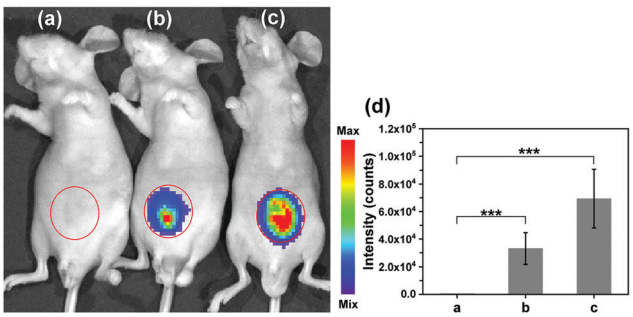

Fig. 6 Fluorescence imaging of thiophenol in nude mice. The mice were injected intraperitoneally with various substances (200 μL): (a) **AQD** (50 μM, 60 min) only; (b) thiophenol (20 μM, 15 min) and then **AQD** (50 μM, 60 min); (c) thiophenol (40 μM, 15 min) and then **AQD** (50 μM, 60 min); (d) fluorescence intensity readout of red circle in (a–c). The excitation filter was 600 nm, and the emission filter was 670 nm.

thus establishing that **AQD** accumulated specifically in the nucleus. Taken together, these solid results evidently indicated that **AQD** can be employed as a robust tool for nuclear thiophenol fluctuation mapping.

Having well-established the thiophenol imaging capability of **AQD** in living cells, an attempt was made to reveal the feasibility of visualizing thiophenol fluctuation *in vivo*. Firstly, the imaging assays in zebrafish were performed. The zebrafish were pretreated with various concentrations of thiophenol and then imaged with **AQD**. As shown in Fig. 5, upon thiophenol administration, the zebrafish exhibited much brighter fluorescence than that imaged in the control group, which was consistent with **AQD**'s fluorescence response behaviors observed in the cells. Afterward, the imaging ability of **AQD** in mice was investigated. The mice were successively given intraperitoneal injection of thiophenol and **AQD**. As illustrated in Fig. 6, almost no distinguishable fluorescence signal was observed in mice treated with **AQD** only. When pre-administrated thiophenol, a notable fluorescent signal increase in a dose-dependent manner was gained, demonstrating that **AQD** is competent to differentiate variations of the thiophenol level in mice. Overall, it is credible to draw the conclusion that **AQD** is capable of monitoring thiophenol fluctuations *in vivo*.

In conclusion, we rationally designed and synthesized a specific fluorescent sensor, **AQD**, for thiophenol tracking in nucleus *via* integrating the dinitrophenyl group into **AQ**. Based on the effective thiolysis of dinitrophenyl ether, **AQD** was capable of capturing thiophenol with outstanding sensitivity and specificity upon PET effect elimination and ICT process recovery. Furthermore, the near-infrared activatable merit of **AQD** endowed its superior fluorescence imaging behaviors *in vitro* and *in vivo*. Therefore, we expect that **AQD** will be a potent candidate for thiophenol research in other physiopathological contexts.

This work was supported by the National Natural Science Foundation of China (91753111, 21927811, 21775093, 21877076, and 21907060) and the Key Research and Development Program of Shandong Province (2018YFJH0502). All animal experiments

were approved by the Animal Care and Use Committee of Shandong Normal University, and were performed in compliance with the Animal Management Rules of the Ministry of Health of the People's Republic of China and the Guidelines for the Care and Use of Laboratory Animals of Shandong Normal University.

Conflicts of interest

There are no conflicts to declare.

Notes and references

1 (*a*) J. C. Love, L. A. Estroff, J. K. Kriebel, R. G. Nuzzo and G. M. Whitesides, *Chem. Rev.*, 2005, **105**, 1103–1170; (*b*) X. Chen, Y. Zhou, X. Peng and J. Yoon, *Chem. Soc. Rev.*, 2010, **39**, 2120–2135.

2 (*a*) F. Wu, H. Wang, J. Xu, H.-Q. Yuan, L. Zeng and G.-M. Bao, *Sens. Actuators, B*, 2018, **254**, 21–29; (*b*) R. Munday, *Free Radical Biol. Med.*, 1989, **7**, 659–673.

3 G. J. Hathaway and N. H. Proctor, *Proctor and Hughes' chemical hazards of the workplace*, John Wiley & Sons, 2014.

4 (*a*) P. Amrolia, S. G. Sullivan, A. Stern and R. Munday, *J. Appl. Toxicol.*, 1989, **9**, 113–118; (*b*) T. R. Juneja, R. L. Gupta and S. Samanta, *Toxicol. Lett.*, 1984, **21**, 185–189; (*c*) R. Munday, *J. Appl. Toxicol.*, 1985, **5**, 409–413; (*d*) M. M. Villalba, V. J. Litchfield, R. B. Smith, A. M. Franklin, N. S. Lawrence and J. Davis, *J. Hazard. Mater.*, 2008, **154**, 444–450.

5 R. P. Verma, S. Kapur, O. Barberena, A. Shusterman, C. H. Hansch and C. D. Selassie, *Chem. Res. Toxicol.*, 2003, **16**, 276–284.

6 (*a*) X. Jiao, Y. Li, J. Niu, X. Xie, X. Wang and B. Tang, *Anal. Chem.*, 2017, **90**, 533–555; (*b*) M. Yang, J. Fan, J. Du and X. Peng, *Chem. Sci.*, 2020, **11**, 5127–5141; (*c*) J. Mei, N. L. Leung, R. T. Kwok, J. W. Lam and B. Z. Tang, *Chem. Rev.*, 2015, **115**, 11718–11940; (*d*) Y. Tang, Y. Ma, J. Yin and W. Lin, *Chem. Soc. Rev.*, 2019, **48**, 4036–4048; (*e*) J. Ohata, K. J. Bruemmer and C. J. Chang, *Acc. Chem. Res.*, 2019, **52**, 2841–2848; (*f*) J. Zheng, R. Yang, M. Shi, C. Wu, X. Fang, Y. Li, J. Li and W. Tan, *Chem. Soc. Rev.*, 2015, **44**, 3036–3055; (*g*) J. A. Robson, M. Kubankova, T. Bond, R. A. Hendley, A. J. P. White, M. K. Kuimova and J. Wilton-Ely, *Angew. Chem., Int. Ed.*, 2020, **59**, 21431–21435; (*h*) J. Niu, J. Fan, X. Wang, Y. Xiao, X. Xie, X. Jiao, C. Sun and B. Tang, *Anal. Chem.*, 2017, **89**, 7210–7215; (*i*) Y. Li, Y. Shu, M. Liang, X. Xie, X. Jiao, X. Wang and B. Tang, *Angew. Chem., Int. Ed.*, 2018, **57**, 12415–12419.

7 (*a*) W. Jiang, Q. Fu, H. Fan, J. Ho and W. Wang, *Angew. Chem., Int. Ed.*, 2007, **46**, 8445–8448; (*b*) J. Hong, Q. Xia, W. Feng and G. Feng, *Dyes Pigm.*, 2018, **159**, 604–609; (*c*) Q. Zhai, S. Yang, Y. Fang, H. Zhang and G. Feng, *RSC Adv.*, 2015, **5**, 94216–94221; (*d*) H. Ren, F. Huo, Y. Huang, J. Chao, W. Wen, J. Fan and C. Yin, *Dyes Pigm.*, 2020, **181**, 108567; (*e*) Z. Li, C. Liu, C. Yu, R. Yuan, P. Jia, Z. Wang, Q. Duan, H. Zhu, B. Zhu and W. Sheng, *New J. Chem.*, 2019, **43**, 6746–6752; (*f*) H. W. Liu, X. B. Zhang, J. Zhang, Q. Q. Wang, X. X. Hu, P. Wang and W. Tan, *Anal. Chem.*, 2015, **87**, 8896–8903; (*g*) Q. Liu, A. Li, X. Li, B. Li, Y. Zhang, J. Li and Y. Guo, *Sens. Actuators, B*, 2019, **283**, 820–830; (*h*) W. Lin, L. Long and W. Tan, *Chem. Commun.*, 2010, **46**, 1503–1505; (*i*) W. Jiang, Y. Cao, Y. Liu and W. Wang, *Chem. Commun.*, 2010, **46**, 1944–1946.

8 (*a*) K. L. Njoh, L. H. Patterson, M. Zloh, M. Wiltshire, J. Fisher, S. Chappell, S. Ameer-Beg, Y. Bai, D. Matthews, R. J. Errington and P. J. Smith, *Cytometry, Part A*, 2006, **69**, 805–814; (*b*) H. D. Ou, S. Phan, T. J. Deerinck, A. Thor, M. H. Ellisman and C. C. O'Shea, *Science*, 2017, **357**, 13; (*c*) V. J. Pansare, S. Hejazi, W. J. Faenza and R. K. Prud'homme, *Chem. Mater.*, 2012, **24**, 812–827.

9 (*a*) Y. Hao, Q. Yin, Y. Zhang, M. Xu and S. Chen, *Molecules*, 2019, **24**, 3716; (*b*) Z. Wang, D. M. Han, W. P. Jia, Q. Z. Zhou and W. P. Deng, *Anal. Chem.*, 2012, **84**, 4915–4920.